International Journal of Chemical and Biochemical Sciences
(ISSN 2226-9614)

Journal Home page: www.iscientific.org/Journal.html

Effect of saccharin on the corrosion of Zn, Fe and Zn-Fe in different electrolytes: A detailed experimental and characterization study

S. AMIRAT[1], K. ABDERRAHIM[2**] and J. CREUS[3]*

[1]*Nanomaterials Corrosion and Surface Treatment Laboratory (LNCTS), Badji Mokhtar University, B.P.12-23000, Annaba, Algeria.*

[2]*Surface Engineering Laboratory (L.I.S), Badji Mokhtar University, B.P.12-23000, Annaba, Algeria.*

[3]*Laboratory Of Studies Of Materials In Mediums Aggressive, University La Rochelle, Avenue Michel Crépeau, F-17042 Rochelle Cedex 0, France.*

Abstract

The electro-crystallization process and electrochemical kinetics of Zn, Fe and Zn-Fe in the presence of saccharin in three different solutions at 298K; E_1: $ZnCl_2$=20.48g/l; KCl=180g/l; H_3BO_3=25g/l without and with the concentrations 0.15 and 0.25 g/l of saccharin.E_2: $FeCl_2$=109.30g/l; $C_6H_8O_6$=3.52g/l; KCl=180g/l; H_3BO_3=25g/l without and with the concentrations 0.15 and 0.25 g/l of saccharin. E_3: $ZnCl_2$=20.48g/l ; $FeCl_2$=109.30g/l; $C_6H_8O_6$=3.52g/l; KCl=180g/l; H_3BO_3=25g/l without and with the concentrations 0.15 and 0.25 g/l of saccharin.using potentiodynamic polarization, electrochemical impedance spectroscopy (EIS). The values of these parameters show that: the charge transfer resistance Rct increases up to 1033 Ω.cm2, this is attributed to the formation of a protective film at the metal/solution interface, the decrease in Cdl values up to 0.11. 10^{-3} µF.cm^2 may result from the increase in the thickness of the film formed on the metal surface which may be due to the adsorption of the saccharin molecules at the metal/solution interface or the decrease in the local dielectric constant. The results of the corrosion tests, we can deduce that saccharin allows us to obtain a more protective alloy layer than the one made from baths not containing saccharin. In particular, the deposit obtained at 2.5 A.dm^{-2} in the presence of saccharin seems to have the best corrosion resistance, its surface hardly changing during the various corrosion tests. The morphological study of the deposits and corrosion products obtained was studied by scanning electron microcopy (SEM). X-ray diffraction (XRD) and Raman spectroscopy. The results obtained from experimental studies were in reasonable agreement and confirm the presence of a protective film.

Keywords: EIS, Tafel, corrosion inhibitor, saccharin, alloy Zn-Fe, XDR -SEM- RAMAN characterization.

Full length article **Corresponding Author*, e-mail: *amiratsam@yahoo.fr **abderrahimkarima@hotmail.fr

1. Introduction

Due to their outstanding electrical, thermal; mechanical properties, easy availability, and cost-effectiveness steel and its alloys attracted extensive attention and have been widely used in various industrial fields [1,2]. However, they may prone to corrosion, especially when exposed to severe use condition[3]. Several ways in this regard were applied to improve the corrosion resistance of these materials. Zn plating is one of the most appropriate, fast, and low effective methods for CS steel protection against corrosion especially in the construction, automotive and household appliance industries [4]. Particularly, Zn coating acts as a sacrificial protective layer for the steel structure due the fact that the dissolution rate of Zn is significantly lower than that of steel also the formation of defensive Zn corrosion products in an aggressive medium [5]. According to U.S. Geological Survey in 2013 [6], the Zinc reserves are not abundant; in which a total of 250 million tons are extractable, be it 19 times larger than the current annual consumption, consequently, the development of alternative coatings is required. Researchers have recently found that the Zn-Alloy coating such as Zn-Fe, Zn-Al and Zn-Mg can improve the corrosion resistance of steel [7,8]. Moreover, introducing additives such as glycerol , saccharin and glucose to improve the plating bath's performance is a simple, precise, and effective method due to the fact that the additive does not only promote the throwing ability of plating baths but also increases the bath's stability and conductivity [9,10]. Whereas, the addition of a suitable additive can enhance the

microstructural, mechanical, and electrochemical properties of Zn and/or Zn-alloy coatings [11].

Electro-crystallization evolution and electrochemical kinetics is considered in this manuscript as the science and technology of obtaining a solid metal deposit at the cathode of an electrolysis cell. A large number of parameters influence the type of deposit: the current density current i; the concentration of metal ions to be discharged CMe^{z+}; the agitation; the temperature; the pH; the presence of other cations and anions; complexation; additives; and substrate,

The objective of this work is to study the effect of saccharin to the corrosion of Zn, Fe and Zn-Fe alloy at different electrolytes by following their electro-crystallization processes and electrochemical kinetics by potentiodynamic polarization method and electrochemical impedance spectroscopy (EIS) as well as characterization methods.

2. Materials and methods

2.1. Materials and electrolytes

The steel studied is an ordinary E24 steel whose chemical composition, established by the XRF (X-ray fluorescence spectrometry) method, is shown in Table 1.

Table 1. Chemical composition of the E24 steel

Element	C	S	Mn	P	N	Fe
M (mass %)	0.17	0.045	1.4	0.045	0.009	98.3

- ✓ The additive tested is saccharin, supplied by the company Sigma-Aldrich and whose chemical structure is presented in Figure 1.

- ✓ The chemical composition of the three electrolytes used is as follows:

E_1: $ZnCl_2$=20.48g/l; KCl=180g/l; H_3BO_3=25g/l

without and with the concentrations 0.15 and 0.25 g/l of saccharin.

E_2: $FeCl_2$=109.30g/l; $C_6H_8O_6$=3.52g/l; KCl=180g/l; H_3BO_3=25g/l without and with the concentrations 0.15 and 0.25 g/l of saccharin.

E_3: $ZnCl_2$=20.48g/l ; $FeCl_2$=109.30g/l; $C_6H_8O_6$=3.52g/l; KCl=180g/l; H_3BO_3=25g/l without and with the concentrations 0.15 and 0.25 g/l of saccharin.

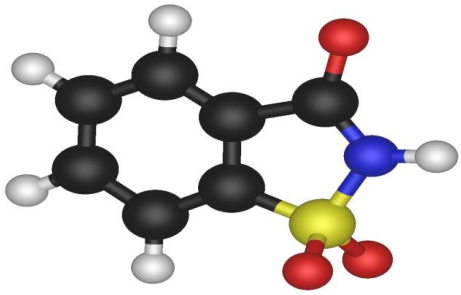

Fig. 1. chemical structure of saccharin ($C_7H_5NO_3S$).

2. 2. Electrochemical measurements

The electrochemical measurements were carried out using a potentiostat / galvanostat, brand voltalab PGZ 301 , associated with a volta-master software and equipped with a classical electrochemical cell with three electrodes: reference electrode (Er) in saturated calomel (SCE), counter electrode in platinum and a working electrode (Et) in E24 steel. This last one is coated in an epoxy resin delimiting a flat working surface of 1cm^2, successively polished with silicon carbide (SiC) abrasive papers at different granulometries: 800, 1200, 2400 and 4000. The steel surface was activated by hydrochloric acid (HCl 50% by volume) for 10s after which it was washed with distilled water, degreased with ethanol in an ultrasonic bath, then washed again with distilled water and finally dried under a dry air flow.

Electrochemical measurements were made after 1h of immersion at 298K:

- ✓ The polarization curves are plotted by sweeping the potential range (-800 to -1600) mV/ SCE at a speed of 20 mV/s.
- ✓ Electrochemical impedance spectroscopy (EIS) measurements were performed in the frequency range from 100 kHz to 10 mHz, with a signal amplitude of 5 mV.

2. 3. Surface analysis

The surface morphology of the Zn-Fe alloys obtained in the absence and presence of saccharin was studied using a JEOL JSM-54 scanning electron microscope, coupled to an energy dispersive spectrometer (EDS).

3. Results and discussions

3. 1. Electrochemical potentiodynamic polarization measurement

3.1.1. Electro reduction of Zn

The monitoring of the electro-reduction process of Zn in solution ($ZnCl_2$=20.48g/l; KCl=180g/l; H_3BO_3=25g/l) in the absence and presence of different concentrations of saccharin at 298 K, is presented in Figure 2. In the absence of saccharin: the negligible cathodic current can be attributed to the discharge of the first zinc seeds on the glassy carbon.
In the presence of saccharin we observe a plateau reflecting the deposition of Zn in the diffusion limit regime is more marked in the interval (-0.95/-1.05 V). Beyond the value -

1.05V we have a slight increase in the cathodic current reflecting the massive deposition of Zn.
In chloride environments, the deposition process of zinc by the reduction of a complex is according to the following reaction [12]:

$$[Zn\ Cl_4]^{2-} + 2\ e^- \longrightarrow Zn + 4Cl^-$$

3.1.2. Electro reduction of Fe

The monitoring of the electro-reduction process of Fe immersed in the solution ($FeCl_2$=109.30g/l; $C_6H_8O_6$=3.52g/l; KCl=180g/l; H_3BO_3=25g/l) without and with the concentrations 0.15 and 0.25 g/l of saccharin after 1 hour of immersion at 298 K, is presented in Figure 3.
From Figure 3 and in the presence of saccharin we notice two changes in slope:

- the first one at -0.9V reflects the reduction of Fe (II) ions.
- the second at -1.3V corresponds to the reduction of H+ ions according to the following mechanism**[13]**:

$$Fe^{2+} + OH^- + e^- \longrightarrow FeOH_{ads}$$

$$FeOH_{ads} + H^+ + e^- \longrightarrow Fe + H_2O$$

In this case the addition of saccharin accelerates the electro-crystallization process.

3.1.3. Electro reduction of Zn-Fe

The monitoring of the electro-reduction process of the Zn-Fe alloy immersed in the solution ($ZnCl_2$=20.48g/l; $FeCl_2$=109.30g/l; $C_6H_8O_6$=3.52g/l; KCl=180g/l; H_3BO_3=25g/l) without and with the concentrations 0.15 and 0.25 g/l of saccharin after 1 hour of immersion at 298 K, is presented in figure 4. According to figure 4 we notice a sudden increase of the current from - 1.1 V/ SCE translating to the discharge of Fe^{2+} and Zn^{2+}. The saccharin therefore inhibits the electro-crystallization of Zn-Fe and also the release of hydrogen.

3.2 Electrochemical impedance spectroscopy measurements (EIS)

To understand the protective mechanisms taking place on the surface of E24 steel in the three different electrolytes (E_1, E_2 and E_3), in the absence and presence of saccharin at different concentrations. We have plotted electrochemical impedance diagrams in Nyquist and bode representation after 1 hour of immersion at 298 K. We notice the presence of a single semicircular capacitive loop, whose size increases with increasing saccharin concentration, due to the progressive formation of a protective film on the surface of the Zn-Fe electrode; this process is controlled by the charge transfer phenomenon (Figure 5.a-a'). as well as the appearance of a resistive region at high frequencies (Figure 5.b-b') [14,15].

The equivalent electrical circuit (EEC), obtained with the help of a simulation software EC-lab, is shown in Figure 6. The values of the different parameters, taken from the parametric fit are grouped in Table 2. The values of these parameters show that: the charge transfer resistance Rct increases up to 1033 Ω.cm2, this is attributed to the formation of a protective film at the metal/solution interface, [17]; the decrease in Cdl values up to 0.11. 10^{-3} µF.cm^2 may result from the increase in the thickness of the film formed on the metal surface which may be due to the adsorption of the saccharin molecules at the metal/solution interface or the decrease in the local dielectric constant [18].

3.3. Surface Analysis

Figure 7 shows the micrographs of the surface of the Zn-Fe alloy, obtained by SEM in E_3 in the absence and presence of 0.25g/l of saccharin and at a current density of 2.5 A.dm-²; without additive (Fig. 7(a)), a very tormented nodular type morphology is obtained for the deposit made in the bath; with additive (Fig. 7(b)), it presents a smooth aspect and a considerable refinement of the morphology of the crystals is observed. These results confirm the adsorption of saccharin molecules on the surface of the samples.

3.4. Study of the corrosion products

The X-ray diffractograms of the Zn-Fe alloy recorded on a BRUKER AXS D8 diffractometer are adjusted by Maud software after a potentiodynamic corrosion test (Fig. 8(a, a') and (b, b')), allows to identify the different phases. At equal current density, and after subjecting the samples to a potentiodynamic corrosion test, it appears that only one corrosion product can be observed: a zinc chlorohydroxide of the formula $ZnCl_2$,4$Zn(OH)_2$, denoted ZHC. In the presence of saccharin Fig.8(b), the phases observed for a non-oxidized deposit are found (pure zinc phase and alloy phase) in addition to the ZHC phase. In the absence of saccharin Fig.8(a), the same ZHC phase is observed but we also observe a phase of the alloy, not present before corrosion .This can be explained by the fact that the X-ray diffraction analysis before corrosion was performed in symmetrical mode while the one after corrosion was performed in fixed and grazing incidence**[13]**.We can thus deduce a certain heterogeneity of the deposit in thickness, the grazing incidence allowing to observe only the superficial layer of the deposit whereas the symmetry mode allows a more in-depth analysis. After the long term corrosion test, Fig 8(a' and b'), only the $ZnCl_2$,4$Zn(OH)_2$ phase (noted ZHC) appears in addition to the phases observed under the same conditions before corrosion. Identical observations can be made for deposits made at a current density of 2.5A.dm^{-2}). Whatever the corrosion test, long term immersion or potentiodynamic, it seems that the phase has completely disappeared and that the only corrosion product is $ZnCl_2$,4$Zn(OH)_2$. It should be noted, however, that other corrosion products are likely to be present without being observable by X-ray diffraction.

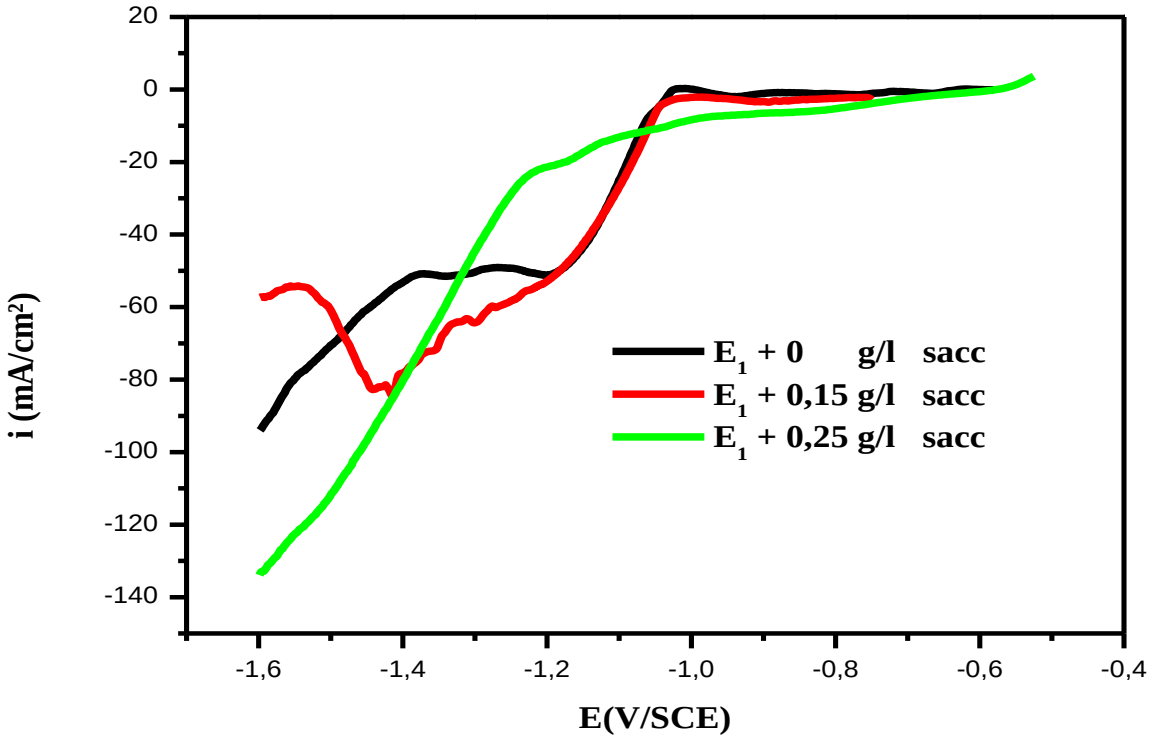

Fig. 2. polarization curves of E24 steel in E_1 in the absence and presence of different concentrations of saccharin.

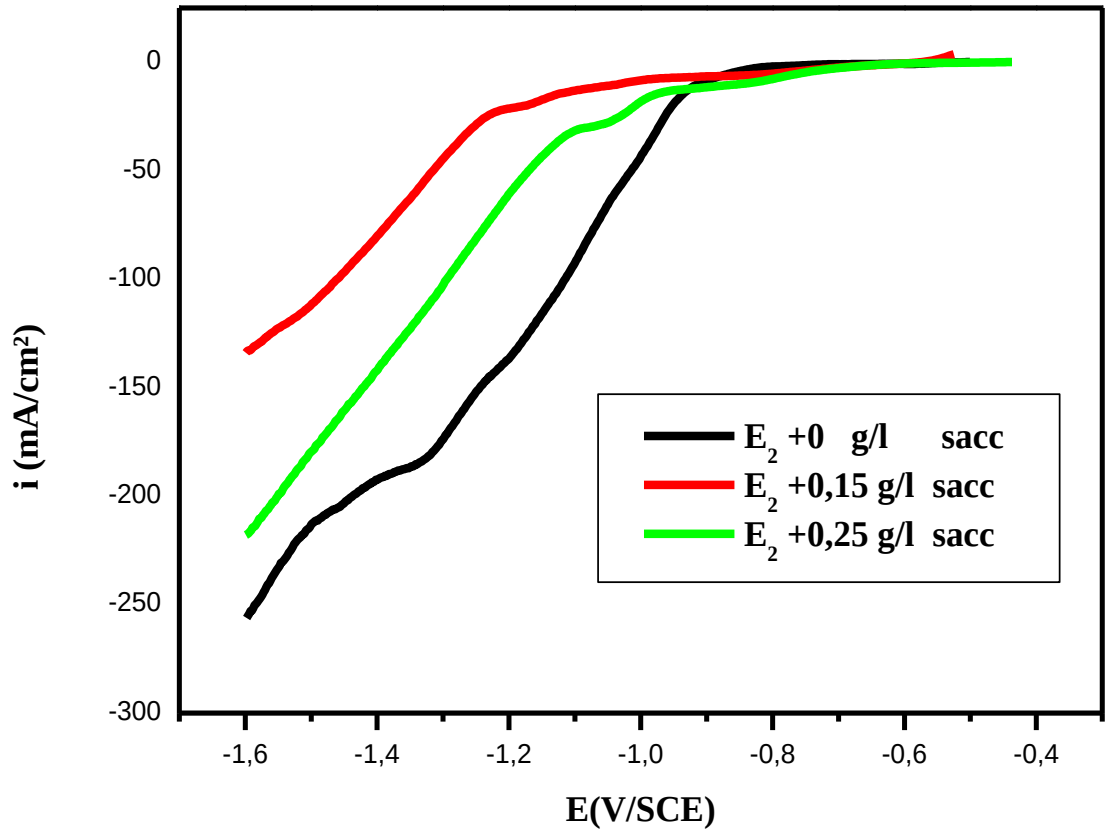

Fig. 3. Polarization curves of E24 steel in E_2 in the absence and presence of different concentrations of saccharin.

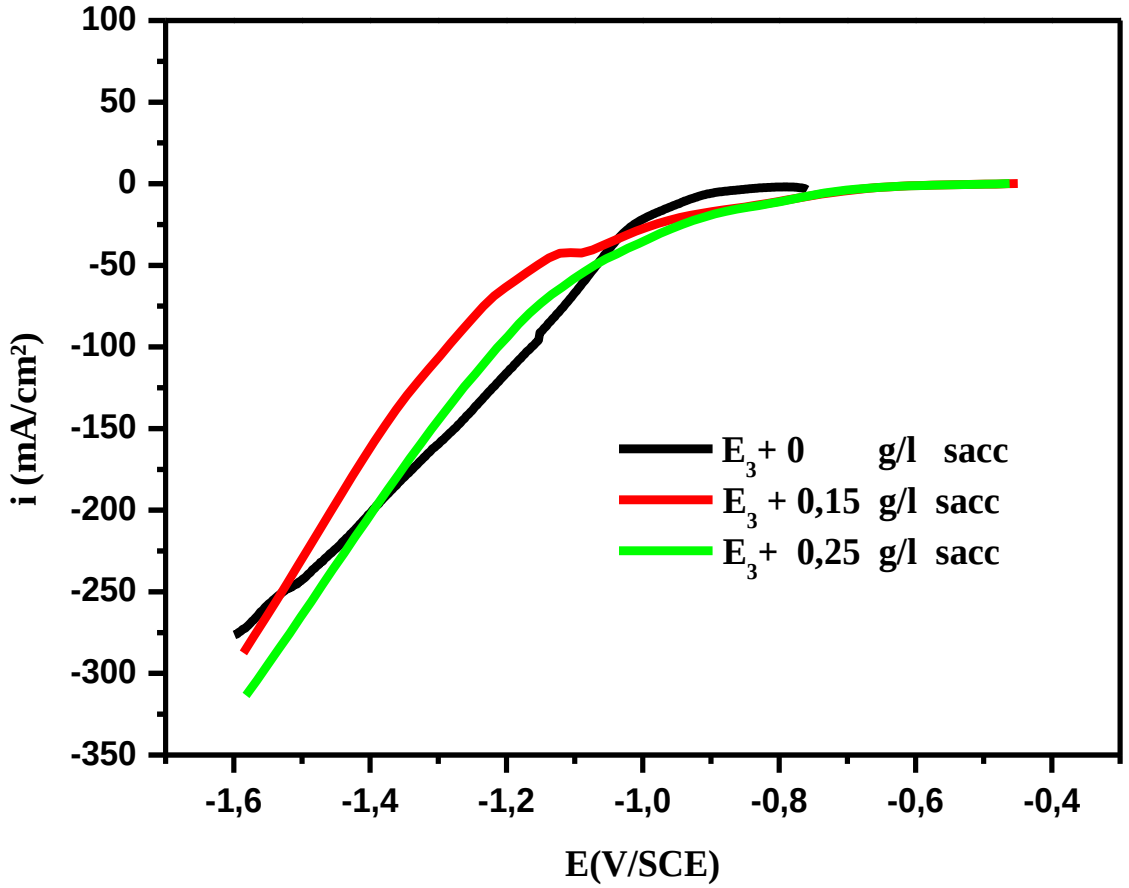

Fig. 4. Polarization curves of E24 steel in E3 in the absence and presence of different concentrations of saccharin.

Table 2. Electrochemical parameters, obtained by EIS, and of Fe, Zn and Zn-Fe steel without and with different concentrations of saccharin.

Elements	Re ($\Omega.cm^2$)	C_{dl} ($\mu F.cm^2$).10^{-3}	α	Rct ($\Omega.cm^2$)
Fe	2.07	0.22	0.70	776
Fe+ 0.25g/l saccharin	1.31	0.82	0.69	68.95
Zn	1.47	0.86	0.69	123
Zn+ 0.25g/l saccharin	1.48	0.84	0.76	51.24
Zn-Fe	1.07	0.15	0.80	291
Zn-Fe+0.25g /l saccharin	1.87	0.11	0.88	1033

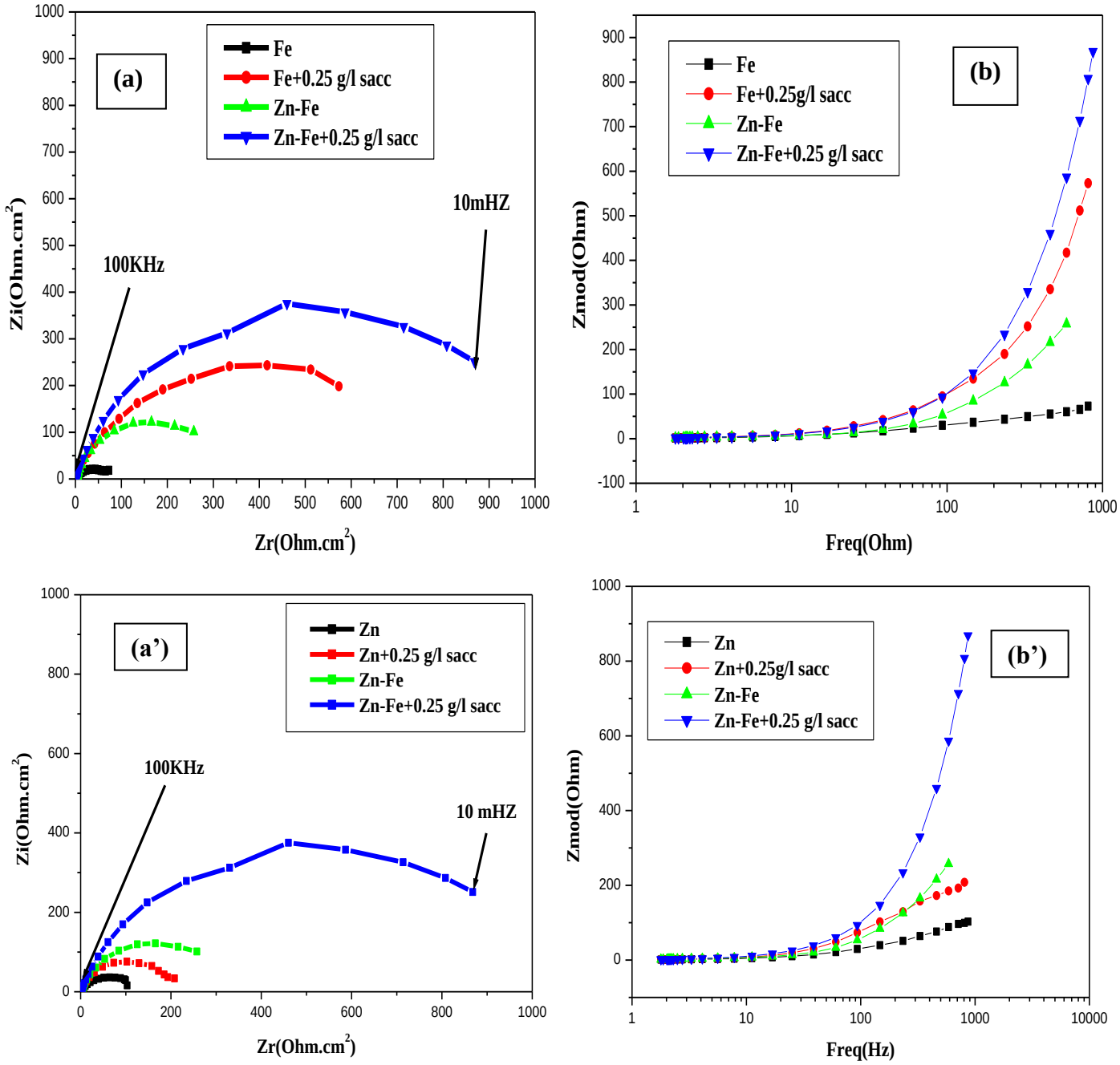

Fig. 5. Nyquist diagrams (a,a'), Bode modulus (b,b') of Fe, Zn and Zn-Fe in different electrolytes without and with saccarin concentrations at 298 K.

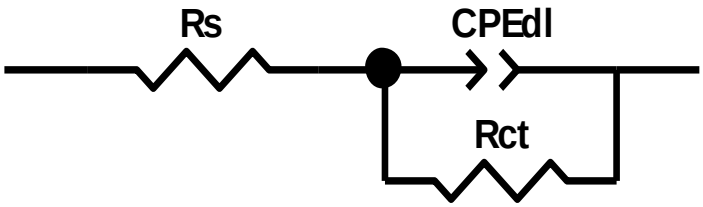

Fig. 6. Equivalent electrical circuit of Fe, Zn and Zn-Fe in E_2 in the absence and presence of saccarin at different concentrations**[16]**.

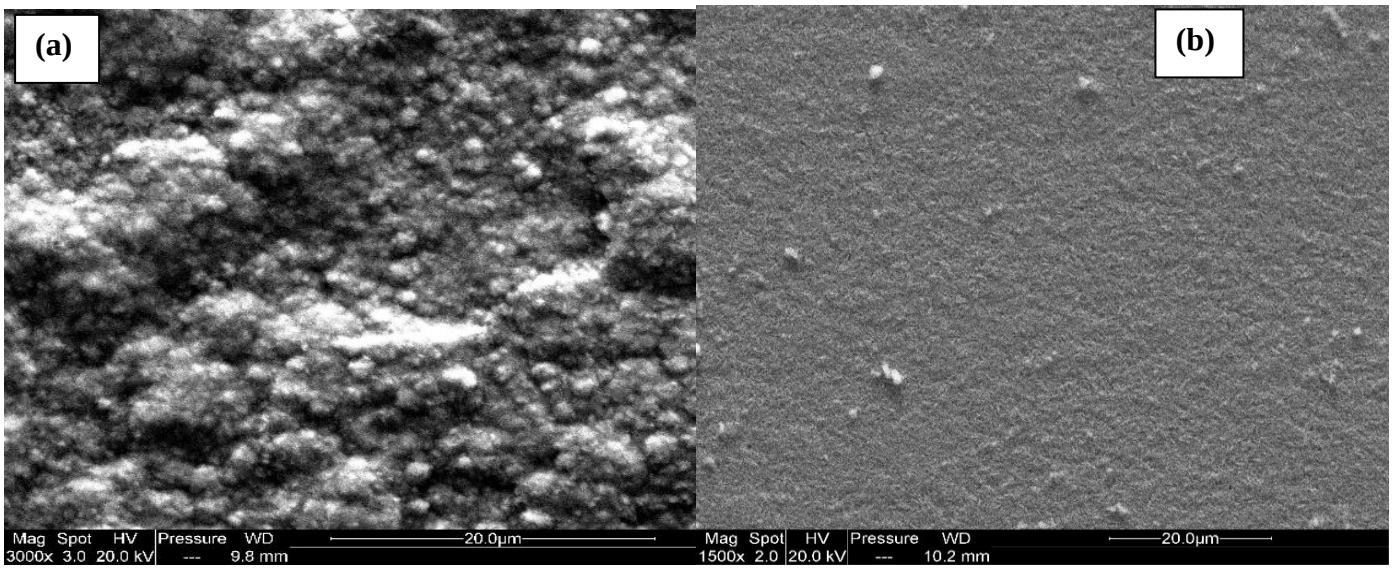

Fig.7. SEM images of E24 steel in E_3, (a) without saccharin, (b) in presence of 0.25g/l saccharin.

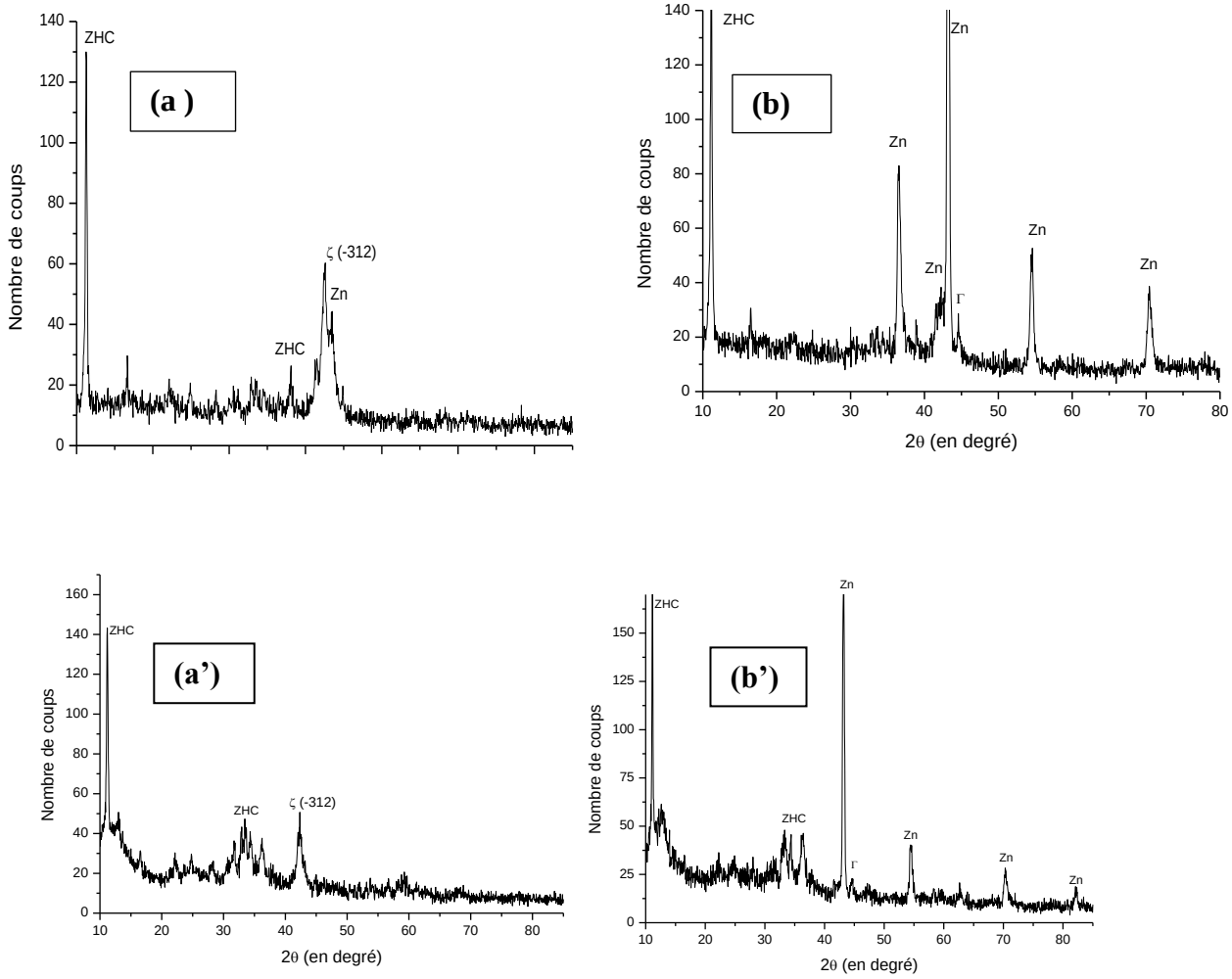

Fig.8. X-ray diffractograms of a Zn-Fe alloy (a,b) deposited at 2.5A/dm^2 ,(a',b') deposited at 1.5A/dm^2 in a bath without and with saccharine subjected to a potentiodynamic corrosion test.

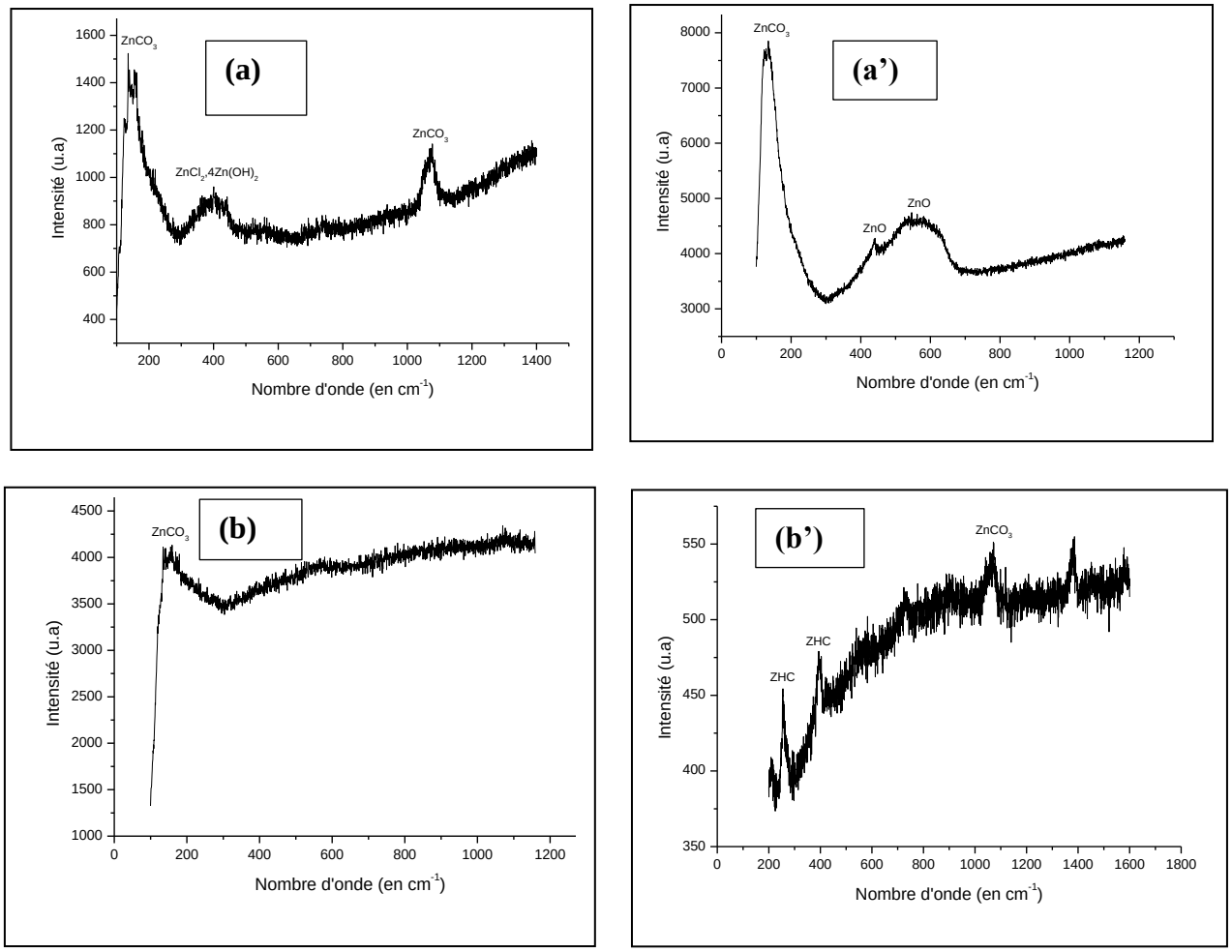

Fig.9. Raman spectra of a Zn-Fe deposit carried out at 1.5 and 2.5 A.dm^{-2} in a bath (a,a') without saccharine, (b,b') in the presence of 0.25g/l saccharine.

Indeed, this method allows to observe only the compounds having a crystalline structure, the amorphous compounds are not observable with this technique. From the Raman spectra, the different corrosion products formed during the long immersion can be determined. It follows that in the presence of saccharin (Figure 9(b,b')), three different corrosion products are obtained: $ZnCO_3$, ZnO and $ZnCl_2$,4Zn(OH)$_2$ (denoted ZHC). Without saccharin, only two corrosion products are present, ZnCO3 and $ZnCl_2$,4Zn(OH)$_2$ (Figure 9 (a,a')). It seems that $ZnCO_3$ and $ZnCl_2$,4Zn(OH)$_2$ are protective in a saline environment but that the presence of ZnO induces a better protection considering the results obtained in potentiodynamics for deposits made in the presence of saccharin. Indeed, these, and in particular the one obtained for a current density of 2.5A.dm^{-2}, have a lower corrosion current density than the deposits obtained for a bath without saccharin. Deposits made in the presence of saccharin would thus present a better protection for the substrate.

4. Conclusions

The study of the effect of saccharin on the electro-crystallization process and the electrochemical kinetics of Zn, Fe and Zn-Fe alloy was evaluated by different methods The following insightful conclusions were made;

- ✓ A negligible cathodic current could be attributed to the discharge of the first zinc seeds on the glassy carbon.
- ✓ The addition of saccharin, inhibits the electro-crystallization process for Zn, but accelerates it for Fe.
- ✓ For the Zn-Fe alloy, a sudden increase of the current was recorded from - 1.1 V/ SCE reflecting the discharge of Fe²+ and Zn2+ ions.
- ✓ Saccharin therefore inhibits the electro-crystallization of Zn-Fe and also the release of hydrogen.
- ✓ Taking into account the results of the corrosion tests, we can deduce that saccharin allows us to obtain a more protective alloy layer than the one made from baths not containing saccharin. In particular, the deposit obtained at 2.5 A.dm^{-2} in the presence of saccharin seems to

have the best corrosion resistance, its surface hardly changing during the various corrosion tests.
As for the addition of saccharin, it inhibits the electro-crystallization process of Zn.

References

[1] M. Missioui, M.B. Idrissi, F. Benhiba, Z. Atioğlu, M. Akkurt, H. Oudda, J.T. Mague, E.M. Essassi, A. Zarrouk, and Y. Ramli.(2022). Synthesis, structural characterization, Hirshfeld surface analysis and anti-corrosion on mild steel in 1M HCl of ethyl 2-(3-methyl-2-oxo-1, 2-dihydroquinoxaline-1-yl) acetate, Journal of Molecular Structure 1251, 132047.

[2] I. Nadi, M. Bouanis, F. Benhiba, K. Nohair, A. Nyassi, A. Zarrouk, C. Jama, and F. Bentiss.(2021). Insights into the inhibition mechanism of 2, 5-bis (4-pyridyl)-1, 3, 4-oxadiazole for carbon steel corrosion in hydrochloric acid pickling via experimental and computational approaches, Journal of Molecular Liquids 342, 116958.

[3] B. Sameh, B. Baya, B. Louiza, H. Soraya, B. Hatem, and B. Merzoug. .(2021). Corrosion inhibition impact of Pyracantha coccinea M. Roem extracts and their use as additives in zinc electroplating: Coating morphology, electrochemical and weight loss investigations, Journal of the Taiwan Institute of Chemical Engineers 121, 337-348.

[4] J.-H. Park, K.-P. Ko, T. Hagio, R. Ichino, and M.-H. Lee. .(2022). Effect of Zn-Mg interlayer on the corrosion resistance of multilayer Zn-based coating fabricated by physical vapor deposition process, Corrosion Science 202, 110330.

[5] S. Anwar, Y. Zhang, and F. Khan.(2018). Electrochemical behaviour and analysis of Zn and Zn–Ni alloy anti-corrosive coatings deposited from citrate baths, RSC advances 8(51): 28861-28873.

[6] U.S. Geological Survey.Mineral commodity summaries. (2013). U. S. Geological Survey; 2013. p. 188–9.

[7] W. Liu, Q. Li, and M.-C. Li.(2017). Corrosion behaviour of hot-dip Al–Zn–Si and Al–Zn–Si–3Mg coatings in NaCl solution, Corrosion Science 121, 72-83.

[8] N. Hosking, M. Ström, P. Shipway, and C. Rudd, Corrosion resistance of zinc–magnesium coated steel, Corrosion science 49(9): 3669-3695.

[9] J.J. Kelly, C. Tian, and A.C. West.(1999). Leveling and microstructural effects of additives for copper electrodeposition, Journal of the Electrochemical Society 146(7) 2540.

[10] D. Nam, R. Kim, D. Han, J. Kim, and H. Kwon. (2011). Effects of $(NH_4)_2SO_4$ and BTA on the nanostructure of copper foam prepared by electrodeposition, Electrochimica Acta 56(25): 9397-9405.

[11] Q. Li, J. Hu, J. Zhang, P. Yang, Y. Hu, and M. An.(2020). Screening of electroplating additive for improving throwing power of copper pyrophosphate bath via molecular dynamics simulation, Chemical Physics Letters 757: 137848.

[12] S. Amirat, R. Rehamnia, M. Bordes and J. Creus. (2013). Materials and Corrosion, Vol 64, Issue 4, 328–334.

[13] S. Amirat, R. Rehamnia, M. Bordes and J. Creus.(2011). Zn–Fe alloy electrodeposition from chloride bath: Influence of deposition parameters on coatings morphology and structure,Materials and Corrosion, 62,No 9999, (2011) 328–334.

[14] K.Abderrahim, O. Mohammad Ahmad Khamaysa, I.Slatnia and H.Zeghache.(2022).Adsorption and performance assessment of 5-Mercapto-1-Methyl Tetrazole as A9M steel corrosion inhibitor in HCl medium: A detailed experimental, and computational methods, chemical data collections 39, 100848.

[15] K. Abderrahim, T. Chouchane, I. Selatnia, A. Sid, and P. Mosset. (2020). Evaluation of the effect of Tetramethylammonium hydroxide on the corrosion inhibition of A9M steel in industrial water: an experimental, morphological and MD simulation insights,chemical data collections 28 (2020) 100391.

[16] K. Abderrahim, I. Selatnia, A. Sid, and P. Mosset.(2018).1,2-bis(4-chlorobenzylidene)Azine as new and effective corrosion inhibitor for copper in 0.1N HCl: A combined experimental and theoretical approach,chemical physics letters 707 (2018)117-128.

[17] P.B. Raja, A.A. Rahim, H. Osman and K. Awang.(2011). Inhibitive effect of Xylopia ferruginea extract on the corrosion of mild steel in 1M HCl medium, Int. J. Miner. Metall. Mater, 18, No.4, p. 413.

[18] I. B. Obot and A. Madhankumar. (2016). Synergistic effect of iodide ion addition on the inhibition of mild steel corrosion in 1 M HCl by 3-amino-2-methylbenzylalcohol, Mater. Chem. Phys, 177(2016), p. 266.

[19] A.J.Bard, and L.R.Faulkner.(2001). Electrochimical methods-Fundamental sand applications, John Wiley& Sons Inc.